doi: 10.1111/j.1365-3121.2005.00609.x

Timing of Late Neoproterozoic glaciation on Baltica constrained by detrital zircon geochronology in the Hedmark Group, south-east Norway

B. Bingen,[1] W. L. Griffin,[2,3] T. H. Torsvik[1,4,5] and A. Saeed[2]

[1]*Geological Survey of Norway, 7491 Trondheim, Norway;* [2]*Department of Earth and Planetary Sciences, GEMOC ARC National Key Centre, Macquarie University, NSW 2109, Australia;* [3]*CSIRO Exploration and Mining, North Ryde, NSW 2113, Australia;* [4]*Institute for Petroleum Technology and Applied Geophysics, NTNU, 7491 Trondheim, Norway;* [5]*School of Geosciences, University of the Witwatersrand, Private Bag 3, PO WITS 2050, Johannesburg, South Africa*

ABSTRACT

The Moelv Tillite is the Late Neoproterozoic Varanger glacial deposit recorded in the Hedmark Group, SE Norway. Paired U–Pb and Lu–Hf data collected on detrital zircons in the Rendalen Formation underlying the Moelv Tillite have identified an uncommon 677 ± 15 to 620 ± 14 Ma population, that constrain the deposition of the Moelv Tillite to be younger than 620 ± 14 Ma. The youngest detrital zircons may be derived from granite magmatism related to the 616 ± 3 Ma Egersund dolerite magmatism, situated in the western part of the Sveconorwegian orogen. The Moelv Tillite, which is not overlain by a cap carbonate, possibly correlates with the *c.* 580 Ma Squantum-Gaskiers glacial deposits of Avalonia. Available palaeomagnetic data for the Late Neoproterozoic suggest that Baltica was located at intermediate to high latitude between 620 and 555 Ma.

Terra Nova, 17, 250–258, 2005

Introduction

Late Neoproterozoic glacial deposits are recorded on most continents (Evans, 2000). Some of these apparently formed at low latitude, implying that the Earth was affected by global glaciations (the 'Snowball Earth' hypothesis; Hoffman and Schrag, 2002), or that the Earth was rotating along a highly oblique axis (the 'high obliquity' hypothesis; Williams, 1975). The synchronicity of glacial deposits is one of the predictions of global glaciation models. Consequently large efforts are being made to improve the stratigraphy and geochronology of sequences containing glacial deposits (Brasier *et al.*, 2000; Thompson and Bowring, 2000; Bowring *et al.*, 2003; Calver *et al.*, 2004; Hoffman *et al.*, 2004; Kendall *et al.*, 2004; Xiao *et al.*, 2004; Zhou *et al.*, 2004). Available data give increasing evidence for at least three major Late Neoproterozoic glaciations, the *c.* 720 Ma Sturtian, *c.* 630 Ma Marinoan and *c.* 580 Ma Gaskiers events.

Correspondence: Bernard Bingen, Geological Survey of Norway, Leiv Eirikssons vei 39, 7491 Trondheim, Norway. Tel.: 00 47 7390 4240; fax: 00 47 7396 1620; e-mail: bernard.bingen@ngu.no.

The Neoproterozoic geological record in Baltica includes a pair of diamictites on the Varanger peninsula in Finnmark in the foreland of the Caledonides (Fig. 1a; Edwards, 1984; Vidal and Moczydlowska, 1995; Harland, 1997). The youngest one represents a reference horizon for the Varanger glaciation (e.g. Hoffman and Schrag, 2002). A diamictite horizon is also reported in sandstone-bearing nappes of the Lower and Middle Allochthons of the Caledonides, the so-called 'sparagmite nappes' (Kumpulainen and Nystuen, 1985). Glacial deposits on Baltica are not reliably dated. Consequently, correlation of the Varanger glacial deposits with Neoproterozoic glacial deposits recorded on other continents is purely speculative.

As part of a study on the Neoproterozoic sediment record of Baltica, we analysed zircons in 10 samples of clastic sediments. An unanticipated but significant Late Neoproterozoic detrital component was detected in one of the samples giving a unique maximum age constraint of 620 ± 14 Ma for deposition of the Moelv Tillite situated in the Hedmark Group of the Lower Allochthon (Fig. 1b). The data lead to a discussion on the geochronology and palaeogeography of the Varanger glaciation on Baltica.

The Hedmark Group

The *c.* 3.5 km thick, weakly deformed, Hedmark Group is exposed in the Osen-Røa Nappe Complex of the Lower Allochthon (Fig. 1a,b; Bjørlykke *et al.*, 1976; Nystuen and Sæther, 1979; Nystuen, 1981, 1987; Vidal and Moczydlowska, 1995). It is characterized by important lateral variations in thickness and facies. Marine turbidites of the Brøttum Formation form the base of the group in the south. In the north-east, the correlative >2 km thick Rendalen Formation consists of fluviatile, braided stream, arkosic sandstone and conglomerate. The Brøttum and Rendalen Formations are overlain by shale and limestone of the Biri Formation, and proximal fluviatile sandstone to conglomerate of the Ring Formation.

The <30 m thick Moelv Tillite caps the Rendalen, Biri and Ring formations, with a possible hiatus. It is composed of glacial diamictite and glaciomarine laminated shale with ice-dropped stones. The Moelv Tillite is everywhere covered by a conformable, transgressive, generally 30–40 m thick, shale horizon, the Ekre Formation. Where exposed, the transition between the diamictites and shale is characterized by a gradual decrease in the grain size of large clasts and

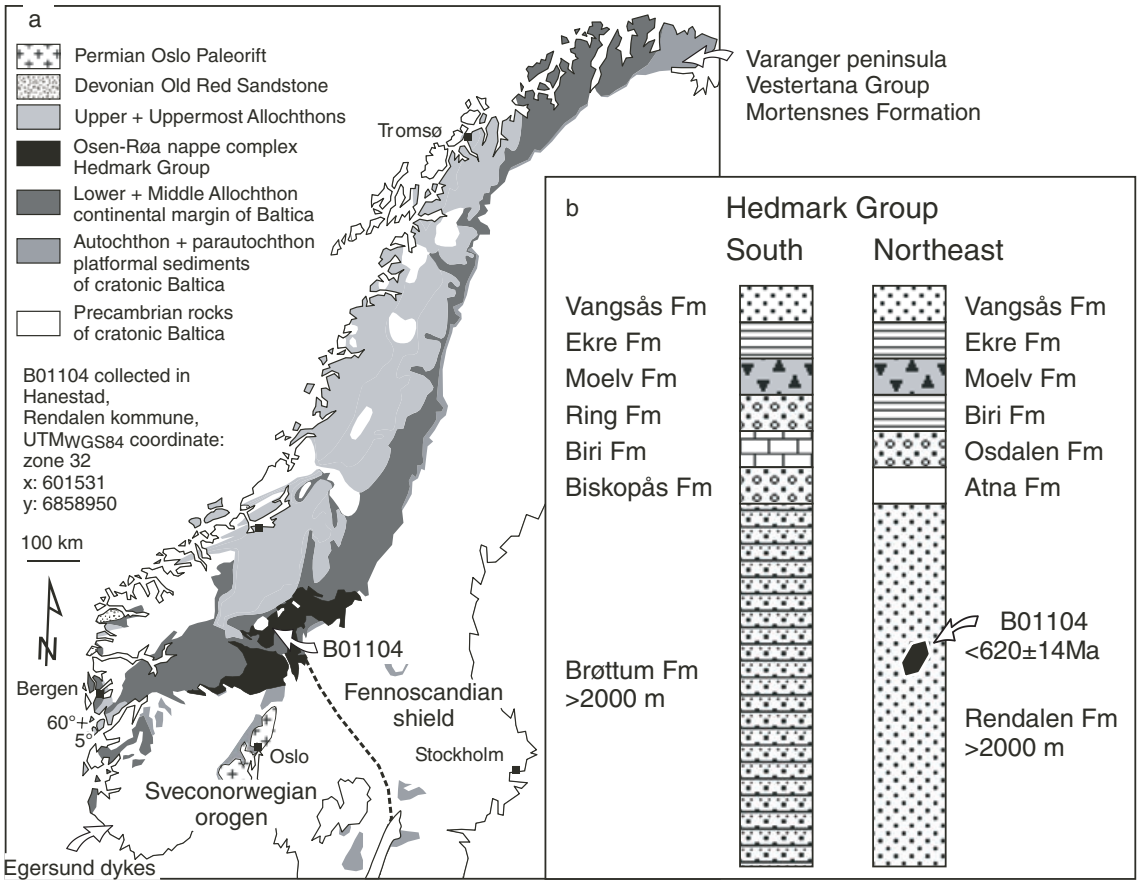

Fig. 1 (a) Simplified tectonostratigraphic map of Scandinavia showing the location of the Hedmark Group and sample locality. (b) Simplified stratigraphic columns for the Hedmark Group in the southern and north-eastern parts of the Osen-Røa Nappe Complex (Bjørlykke *et al.*, 1976; Kumpulainen and Nystuen, 1985; Nystuen, 1987; Vidal and Moczydlowska, 1995).

matrix (Bjørlykke *et al.*, 1976). The youngest exposed Vangsås Formation is overlain by a fossiliferous transgressive Cambrian sequence.

Results

Sampling and U–Pb analyses

Sample B01104 is a typical fluviatile facies of the Rendalen Formation collected in Hanestad (Fig. 1a). The outcrop is poorly bedded arkose, showing common green to red shale interbeds and cobbles. The sample is a poorly sorted coarse-grained (*c.* 1 mm) arkose ($SiO_2 = 81.3$ %) showing subangular clasts in a silt matrix. Detrital zircons are prismatic to rounded, and variably abraded and fragmented because of transportation.

Analytical work on zircon was performed at the Department of Earth and Planetary Sciences, Macquarie University. Non-magnetic zircons were mounted in epoxy. They were imaged and analysed for Si, Zr, Hf, and Y in an electron microprobe. More than 95% of the zircons display magmatic prism-parallel oscillatory zoning. U–Th–Pb geochronological analyses were performed with laser ablation inductively coupled plasma quadrupole mass spectrometry (ICPMS) on 73 crystals (Table 1). Analytical procedures, standardization, data reduction, error propagation and common-Pb corrections are summarized in Belousova *et al.* (2001) and Jackson *et al.* (2004). The age selected for geological interpretation is the $^{207}Pb/^{206}Pb$ age for zircons older than 1000 Ma and the $^{238}U/^{206}Pb$ age for younger zircons.

All but two of the analysed zircons yield concordant to near-concordant U–Pb analyses ranging from 1839 ± 54 to 985 ± 18 Ma (65 grains, 2σ uncertainty) and from 685 ± 28 to 611 ± 26 Ma (six grains; Fig. 2a). The probability density plot of ages show peaks at 1606 ± 36, 1483 ± 35, 1302 ± 57, 985 ± 18, 677 ± 15 and 620 ± 14 Ma (Fig. 2b). The peak at 1.48 Ga largely dominates the distribution. The youngest peak is defined by the weighted average $^{206}Pb/^{238}U$ age of overlapping analyses on two grains. The grain at 611 ± 26 Ma is a non-abraded, U-poor (24 ppm), weakly oscillatory-zoned, prismatic (80 × 250 μm) crystal and the other at 623 ± 16 Ma is a rounded fragment (100 μm in diameter) of a probably large crystal showing oscillatory zoning and a medium U content (167 ppm). Both crystals have typical magmatic Th/U ratios of 0.7–0.8. The moderate U content of these grains, the occurrence of prism-parallel zoning, the concordant behaviour and the absence of significant metamorphic overprint in the rock suggest that the U–Pb systematics have not been affected by

Table 1 LA–ICPMS U–Pb data on detrital zircons, sample B01104, Rendalen Formation.

	Concentrations		Ratios, common-lead corrected								Ages†‡				
No.*	U (ppm)	Th (ppm)	$^{207}Pb/^{206}Pb$	±2σ	$^{207}Pb/^{235}U$	±2σ	$^{206}Pb/^{238}U$	±2σ	$^{208}Pb/^{232}Th$	±2σ	$^{207}Pb/^{206}Pb$ (Ma)	±2σ	$^{206}Pb/^{238}U$ (Ma)	±2σ	Conc§ (%)
57	24	19	0.0594	0.0053	0.834	0.072	0.0994	0.0026	0.0306	0.0026	581	190	**611**	**26**	105
58	167	122	0.0610	0.0013	0.853	0.015	0.1014	0.0017	0.0313	0.0005	640	44	**623**	**16**	97
27	111	52	0.0627	0.0014	0.903	0.019	0.1044	0.0020	0.0329	0.0007	699	48	**640**	**18**	92
59	74	54	0.0587	0.0025	0.875	0.033	0.1076	0.0020	0.0333	0.0010	556	90	**659**	**18**	119
44	101	47	0.0627	0.0016	0.956	0.023	0.1107	0.0023	0.0343	0.0008	697	52	**677**	**20**	97
56	18	12	0.0624	0.0037	0.964	0.055	0.1120	0.0032	0.0338	0.0018	686	124	**685**	**28**	100
52	272	5	0.0720	0.0014	1.638	0.028	0.1651	0.0029	0.0518	0.0016	985	40	**985**	**18**	100
47	37	4	0.0690	0.0026	1.644	0.051	0.1713	0.0035	0.0518	0.0050	898	76	1019	20	113
19	53	73	0.0776	0.0036	2.302	0.096	0.2130	0.0043	0.0638	0.0026	**1136**	**90**	1245	20	110
20	19	10	0.0788	0.0040	2.379	0.110	0.2162	0.0045	0.0647	0.0038	**1167**	**98**	1262	20	108
13	102	56	0.0823	0.0018	2.385	0.050	0.2103	0.0042	0.0639	0.0013	**1252**	**42**	1230	20	98
84	20	11	0.0828	0.0022	2.284	0.057	0.2003	0.0040	0.0607	0.0015	**1264**	**52**	1177	20	93
3	514	128	0.0829	0.0026	2.662	0.068	0.2302	0.0044	0.0686	0.0032	**1267**	**62**	1336	18	105
41	73	56	0.0844	0.0018	2.692	0.056	0.2313	0.0046	0.0690	0.0013	**1302**	**42**	1342	20	103
2	46	36	0.0848	0.0030	2.630	0.080	0.2240	0.0038	0.0665	0.0021	**1311**	**66**	1303	18	99
26	5	3	0.0855	0.0059	2.718	0.178	0.2306	0.0078	0.0710	0.0051	**1327**	**130**	1338	34	101
71	61	34	0.0858	0.0018	2.727	0.056	0.2306	0.0045	0.0689	0.0013	**1333**	**42**	1338	20	100
25	4	5	0.0859	0.0051	2.692	0.152	0.2274	0.0067	0.0668	0.0031	**1335**	**114**	1321	30	99
62	35	27	0.0871	0.0034	2.757	0.094	0.2289	0.0044	0.0678	0.0024	**1362**	**74**	1328	20	98
14	19	18	0.0885	0.0067	3.250	0.228	0.2515	0.0070	0.0739	0.0091	**1393**	**142**	1446	28	104
4	97	76	0.0887	0.0020	2.876	0.062	0.2348	0.0047	0.0690	0.0014	**1397**	**42**	1360	20	97
7	84	146	0.0893	0.0019	3.224	0.062	0.2619	0.0047	0.0724	0.0012	**1410**	**42**	1499	18	106
24	138	87	0.0912	0.0020	3.291	0.073	0.2619	0.0055	0.0770	0.0017	**1450**	**42**	1499	22	103
49	5	12	0.0914	0.0050	3.122	0.161	0.2476	0.0074	0.0685	0.0024	**1456**	**102**	1426	30	98
55	42	36	0.0915	0.0019	3.130	0.057	0.2481	0.0043	0.0751	0.0013	**1456**	**40**	1429	18	98
54	43	36	0.0918	0.0020	3.211	0.060	0.2535	0.0044	0.0771	0.0014	**1464**	**42**	1457	18	100
77	68	38	0.0919	0.0019	3.232	0.064	0.2553	0.0049	0.0715	0.0013	**1465**	**40**	1466	20	100
73	245	187	0.0921	0.0037	3.230	0.111	0.2525	0.0054	0.0743	0.0027	**1469**	**76**	1451	22	99
61	79	55	0.0921	0.0020	3.226	0.058	0.2540	0.0042	0.0749	0.0013	**1470**	**40**	1459	16	99
11	58	41	0.0924	0.0021	3.241	0.070	0.2544	0.0051	0.0855	0.0018	**1475**	**42**	1461	20	99
6	22	47	0.0925	0.0024	3.288	0.071	0.2578	0.0044	0.0737	0.0013	**1477**	**48**	1479	18	100
30	54	66	0.0926	0.0020	3.250	0.062	0.2547	0.0046	0.0744	0.0013	**1479**	**40**	1462	18	99
50	607	261	0.0926	0.0018	3.304	0.065	0.2586	0.0052	0.0784	0.0014	**1480**	**38**	1483	20	100
76	39	90	0.0927	0.0027	3.246	0.097	0.2539	0.0061	0.0709	0.0016	**1482**	**56**	1459	24	98
16	61	79	0.0928	0.0020	3.215	0.062	0.2514	0.0047	0.0745	0.0013	**1483**	**40**	1446	18	98
40	58	114	0.0929	0.0020	3.240	0.068	0.2532	0.0050	0.0745	0.0013	**1485**	**40**	1455	20	98
67	116	112	0.0929	0.0019	3.307	0.065	0.2582	0.0049	0.0767	0.0013	**1486**	**40**	1481	20	100
79	65	96	0.0930	0.0020	3.228	0.065	0.2520	0.0049	0.0718	0.0012	**1487**	**40**	1449	20	97
12	286	387	0.0933	0.0019	3.224	0.065	0.2509	0.0050	0.0758	0.0014	**1493**	**38**	1443	20	97
82	20	41	0.0934	0.0026	3.184	0.078	0.2473	0.0047	0.0711	0.0014	**1496**	**52**	1424	20	95
48	17	16	0.0935	0.0023	3.369	0.073	0.2613	0.0048	0.0790	0.0017	**1498**	**46**	1497	18	100
33	49	31	0.0937	0.0021	3.389	0.076	0.2629	0.0055	0.0763	0.0016	**1502**	**42**	1505	20	100

Table 1 Continued

	Concentrations		Ratios, common-lead corrected								Ages†‡				
No.*	U (ppm)	Th (ppm)	$^{207}Pb/^{206}Pb$	±2σ	$^{207}Pb/^{235}U$	±2σ	$^{206}Pb/^{238}U$	±2σ	$^{208}Pb/^{232}Th$	±2σ	$^{207}Pb/^{206}Pb$ (Ma)	±2σ	$^{206}Pb/^{238}U$ (Ma)	±2σ	Conc§ (%)
5	112	110	0.0941	0.0020	3.489	0.066	0.2688	0.0049	0.0777	0.0013	**1510**	**40**	1535	18	102
42	62	51	0.0951	0.0021	3.646	0.077	0.2780	0.0056	0.0802	0.0016	**1531**	**40**	1581	20	103
43	114	94	0.0959	0.0020	3.568	0.058	0.2699	0.0042	0.0798	0.0012	**1545**	**38**	1540	16	100
43	110	90	0.0963	0.0020	3.933	0.077	0.2963	0.0057	0.0835	0.0015	**1553**	**38**	1673	20	108
63	171	101	0.0974	0.0020	3.729	0.079	0.2777	0.0058	0.0904	0.0018	**1575**	**38**	1580	20	100
64	35	32	0.0975	0.0025	3.540	0.085	0.2634	0.0054	0.0787	0.0018	**1576**	**48**	1507	20	96
9	49	58	0.0977	0.0021	3.570	0.065	0.2650	0.0046	0.0773	0.0013	**1580**	**40**	1515	18	96
51	22	27	0.0985	0.0022	3.788	0.078	0.2788	0.0053	0.0843	0.0016	**1596**	**42**	1585	20	99
36	44	35	0.0987	0.0024	3.762	0.098	0.2778	0.0065	0.0838	0.0021	**1600**	**46**	1580	24	99
65	33	27	0.0987	0.0023	3.588	0.074	0.2637	0.0047	0.0797	0.0016	**1600**	**44**	1508	18	94
39	183	53	0.0991	0.0021	3.838	0.092	0.2816	0.0065	0.1050	0.0026	**1607**	**40**	1599	24	100
8	90	68	0.0996	0.0020	3.940	0.068	0.2868	0.0048	0.0804	0.0013	**1617**	**38**	1625	16	100
66	95	50	0.0996	0.0021	3.773	0.077	0.2747	0.0055	0.0817	0.0016	**1617**	**38**	1565	20	97
35	331	174	0.0997	0.0020	3.910	0.083	0.2857	0.0062	0.0911	0.0017	**1619**	**38**	1620	22	100
21	260	136	0.1003	0.0021	3.734	0.068	0.2701	0.0047	0.0682	0.0013	**1629**	**40**	1541	18	95
37	202	70	0.1017	0.0021	4.040	0.084	0.2891	0.0060	0.0982	0.0018	**1655**	**38**	1637	20	99
31	101	70	0.1020	0.0021	4.013	0.081	0.2857	0.0056	0.0836	0.0015	**1660**	**38**	1620	20	98
18	30	29	0.1024	0.0028	4.170	0.110	0.2954	0.0064	0.0916	0.0023	**1668**	**50**	1669	22	100
46	18	24	0.1026	0.0024	4.183	0.091	0.2958	0.0058	0.0865	0.0017	**1671**	**42**	1671	20	100
17	116	86	0.1033	0.0022	4.254	0.093	0.2986	0.0063	0.0892	0.0019	**1685**	**40**	1684	22	100
29	196	226	0.1040	0.0021	4.307	0.086	0.3006	0.0059	0.0862	0.0016	**1696**	**38**	1694	20	100
69	116	76	0.1040	0.0022	4.184	0.090	0.2919	0.0062	0.0875	0.0017	**1696**	**38**	1651	22	97
22	112	92	0.1049	0.0022	4.387	0.084	0.3032	0.0055	0.0808	0.0015	**1713**	**40**	1707	18	100
1	234	113	0.1055	0.0021	4.445	0.080	0.3055	0.0055	0.0882	0.0014	**1723**	**36**	1719	18	100
74	74	45	0.1056	0.0024	4.457	0.101	0.3062	0.0064	0.0869	0.0020	**1725**	**42**	1722	20	100
32	114	81	0.1073	0.0022	4.616	0.089	0.3124	0.0060	0.0919	0.0016	**1754**	**36**	1753	20	100
53	85	60	0.1073	0.0021	4.559	0.082	0.3081	0.0056	0.0937	0.0016	**1754**	**36**	1731	18	99
78	148	130	0.1077	0.0022	4.339	0.088	0.2922	0.0059	0.0911	0.0016	**1762**	**38**	1652	20	94
15	122	31	0.1094	0.0025	4.839	0.114	0.3208	0.0071	0.0936	0.0028	**1790**	**42**	1794	22	100
60	164	87	0.1124	0.0034	4.717	0.116	0.3031	0.0055	0.0874	0.0032	**1839**	**54**	1707	18	93
45	119	101	0.1153	0.0024	4.821	0.098	0.3032	0.0061	0.0658	0.0012	1885	36	1707	20	91

*Each identification number represents one detrital zircon crystal, sorted by increasing age

† $\lambda^{238}U = 1.55125 \times 10^{-10}$ yr^{-1}, $\lambda^{235}U = 9.8485 \times 10^{-10}$ yr^{-1}, $^{238}U/^{235}U = 137.88$. Age selected for probability density diagram are outlined in bold.

‡The standard zircon 91500 was analysed as an unknown 11 times during this study, giving a weighted mean $^{207}Pb/^{206}Pb$ age of 1066 ± 13 Ma (95% confidence limit), identical to TIMS data reported by Wiedenbeck *et al.* (1995).

§Concordance: 100*$^{206}Pb/^{238}U$ age/$^{207}Pb/^{206}Pb$ age.

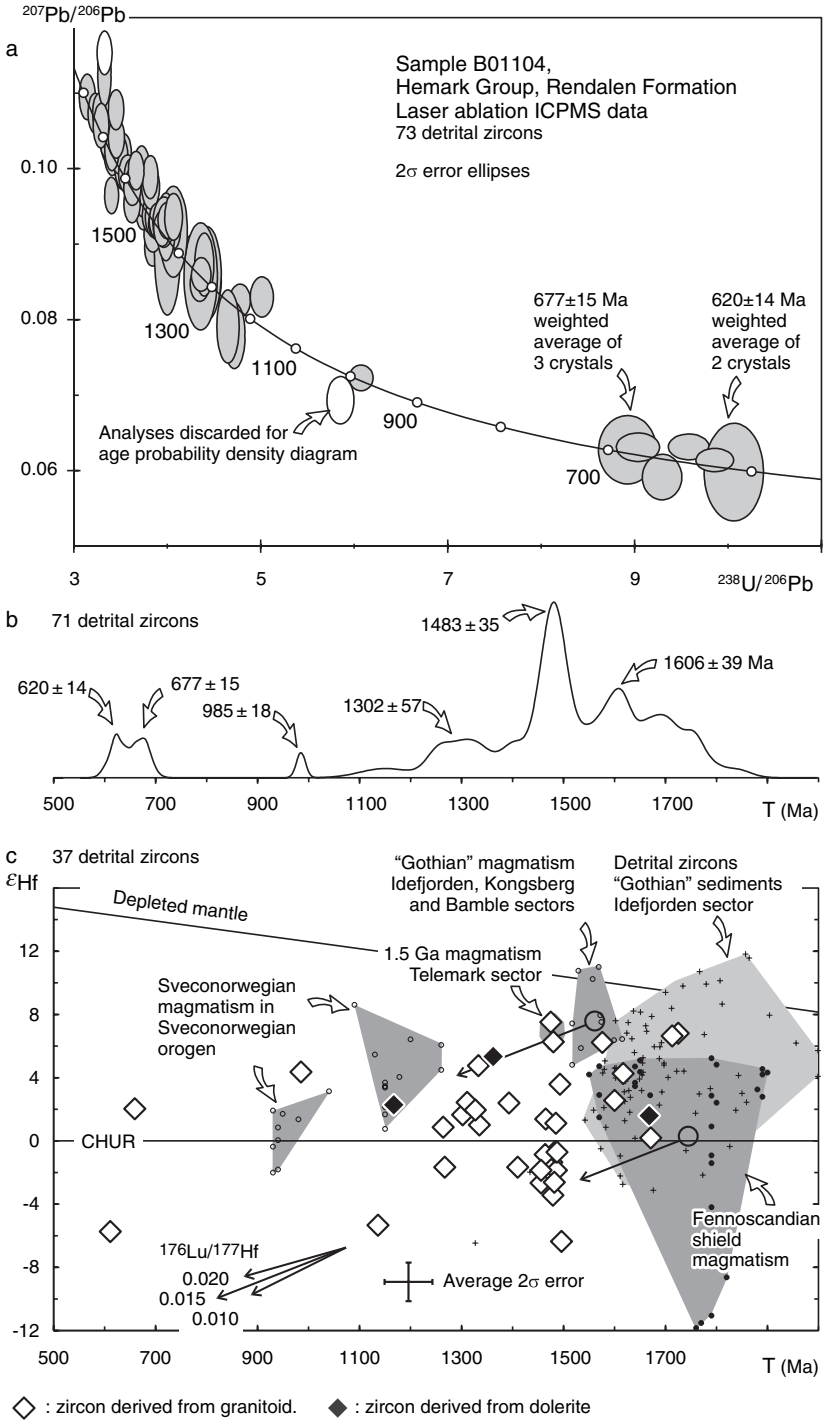

Fig. 2 U–Pb and Lu–Hf data on detrital zircons from sample B01104 of the Rendalen Formation. (a) Concordia diagram. (b) Age probability density diagram following Ludwig (2001). (c) Initial εHf vs. time diagram. Zircons derived from probable granite and dolerite sources are distinguished according to trace element content (U, Th, Y, Yb, Lu and Hf), following the method of Belousova *et al.* (2002). Initial εHf values were calculated using $\lambda^{176}Lu = 1.865 \times 10^{-11}$ yr^{-1} (Scherer *et al.*, 2001). Chondritic reservoir (CHUR) and depleted mantle follow Griffin *et al.* (2000). Regional data in the Sveconorwegian orogen and Fennoscandian shield are from Patchett *et al.* (1981), Vervoort and Patchett (1996) and Andersen *et al.* (2002, 2004). Mesoproterozoic zircon populations of sample B01104 are situated between the growth vectors ($^{176}Lu/^{177}Hf = 0.015$) of the 1.6–1.5 Ga 'Gothian' juvenile magmatism exposed in the central part of the Sveconorwegian orogen and the Palaeoproterozoic magmatic rocks exposed in the east of the Sveconorwegian orogen and in the Fennoscandian shield. The Hf isotopic signature of zircon is consistent with a Baltica provenance for the Rendalen Formation.

post-crystallization Pb loss. Therefore, the age of 620 ± 14 Ma reflects the crystallization of the youngest detected detrital component in the sample, and represents a maximum age for deposition of the sediment.

Sample B01104 was collected from an area where the stratigraphic relationships between the Rendalen and Moelv Formations (Fig. 1b) are verified in a number traverses (Nystuen, 1987). Consequently, the youngest detected detrital zircons in the Rendalen Formation also provide a maximum age of 620 ± 14 Ma for deposition of the overlying Moelv Tillite.

Lu–Hf isotopic analyses

Lu–Hf isotopic analyses were performed on 37 of the dated crystals, wherever the size of the crystal allowed placing two laser ablation pits (Table 2). Analyses were carried out with laser ablation multicollector ICPMS following the method summarized in Griffin *et al.* (2000, 2002). The initial $^{176}Hf/^{177}Hf$ ratio or εHf of the zircon represents an estimate of the isotopic composition of the source rock at the time of crystallization, and helps tracing potential sources for the sediment (Fig. 2c). The main population of Mesoproterozoic detrital zircons at 1.48 Ga encompasses the whole range of Hf isotopic compositions detected in the sample with εHf values between +8 and −6. Two Late Neoproterozoic crystals at 659 and 611 Ma have εHf values of +2 and −6, respectively.

Table 2 LA-ICPMS Lu–Hf data on detrital zircons, sample B01104, Rendalen Formation.

No.*	$^{176}Hf/^{177}Hf$†	±2σ	$^{176}Lu/^{177}Hf$	$^{176}Yb/^{177}Hf$	Age‡	Hfi§	εHf	±2σ
57	0.282237	0.000036	0.000649	0.0346	611	0.282230	−5.7	1.3
59	0.282432	0.000036	0.001052	0.0603	659	0.282419	2.0	1.3
52	0.282281	0.000036	0.000074	0.0037	985	0.282280	4.4	1.3
19	0.281929	0.000036	0.000859	0.0410	1136	0.281911	−5.3	1.3
20	0.282122	0.000040	0.000730	0.0350	1167	0.282106	2.3	1.4
84	0.282012	0.000034	0.000309	0.0140	1264	0.282005	0.9	1.2
3	0.281951	0.000036	0.000821	0.0336	1267	0.281931	−1.7	1.3
41	0.282016	0.000040	0.000550	0.0229	1302	0.282002	1.6	1.4
2	0.282051	0.000034	0.001291	0.0577	1311	0.282019	2.4	1.2
26	0.282022	0.000048	0.001070	0.0498	1327	0.281995	2.0	1.7
71	0.282083	0.000028	0.000495	0.0215	1333	0.282071	4.8	1.0
25	0.281979	0.000030	0.000610	0.0273	1335	0.281964	1.0	1.1
62	0.282085	0.000036	0.000639	0.0312	1362	0.282069	5.3	1.3
14	0.281984	0.000030	0.000687	0.0315	1393	0.281966	2.4	1.1
7	0.281853	0.000030	0.000465	0.0211	1410	0.281841	−1.7	1.1
49	0.281795	0.000050	0.000433	0.0203	1456	0.281783	−2.7	1.8
55	0.281825	0.000034	0.000702	0.0330	1456	0.281806	−1.9	1.2
54	0.281853	0.000030	0.000872	0.0428	1464	0.281829	−0.9	1.1
77	0.281904	0.000028	0.000456	0.0194	1465	0.281891	1.4	1.0
11	0.282075	0.000028	0.000612	0.0265	1475	0.282058	7.5	1.0
6	0.281820	0.000032	0.000480	0.0217	1477	0.281807	−1.4	1.1
30	0.281759	0.000046	0.000443	0.0192	1479	0.281747	−3.4	1.6
50	0.282036	0.000040	0.000593	0.0259	1480	0.282019	6.3	1.4
76	0.281781	0.000022	0.000471	0.0233	1482	0.281768	−2.6	0.8
16	0.281847	0.000038	0.000922	0.0437	1483	0.281821	−0.7	1.3
40	0.281891	0.000032	0.000706	0.0331	1485	0.281871	1.1	1.1
67	0.281805	0.000032	0.000651	0.0280	1486	0.281787	−1.9	1.1
79	0.281839	0.000019	0.000729	0.0337	1487	0.281819	−0.7	0.7
12	0.281970	0.000032	0.001215	0.0532	1493	0.281936	3.6	1.1
82	0.281668	0.000028	0.000510	0.0240	1496	0.281654	−6.4	1.0
64	0.281982	0.000040	0.000831	0.0355	1576	0.281957	6.2	1.4
36	0.281857	0.000048	0.000605	0.0257	1600	0.281839	2.6	1.7
66	0.281899	0.000036	0.000760	0.0298	1617	0.281876	4.3	1.3
18	0.281793	0.000042	0.000793	0.0350	1668	0.281768	1.6	1.5
46	0.281742	0.000034	0.000492	0.0230	1671	0.281726	0.2	1.2
22	0.281901	0.000026	0.000606	0.0274	1713	0.281881	6.6	0.9
74	0.281899	0.000034	0.000627	0.0256	1725	0.281879	6.8	1.2

*Identification number refers to the crystals listed in Table 1.

†Our mean of 293 analyses of $^{176}Hf/^{177}Hf$ in standard zircon 91 500 is 0.282284 ± 30 (2σ), identical to TIMS data reported by Wiedenbeck *et al.* (1995).

‡U/Pb age of the zircon crystal in Ma, following Table 1.

§Initial $^{176}Hf/^{177}Hf$ calculated at the crystallization age with a decay constant of 1.865×10^{-11} yr^{-1}.

Provenance analysis

The Osen-Røa Nappe Complex can be restored to a significantly more westerly position before Caledonian transport (Nystuen, 1981). The comparatively proximal Rendalen Formation sampled a catchment dominated by granitic rocks formed *c.* 1.48 Ga (Fig. 2b). Such rocks are abundant in the western part of the Sveconorwegian orogen (Bingen *et al.*, 2005). The Hf isotopic signature of the zircons is consistent with derivation of source rocks from isotope reservoirs reported in the Sveconorwegian orogen and in the south-west of the Fennoscandian shield (Fig. 2c). The source of the 677 ± 15 to 620 ± 14 Ma zircons is not directly known. However, the 616 ± 3 Ma Egersund dolerite swarm in Rogaland, south Norway (Bingen *et al.*, 1998), attests to mafic magmatism overlapping in age with these zircons, in the probable catchment area of the Rendalen Formation. This rift-related mafic magmatism is characterized by εNd values between +1 and +3 (Bingen and Demaiffe, 1999), and was possibly associated with crustally derived felsic magmas containing zircon. The εHf values at +2 and −6 for the two detrital zircons at 659 and 611 Ma in the Rendalen Formation, are consistent with a provenance from magmatic rocks related to the Egersund event (Fig. 2c). The local occurrence of lenticular bodies of basalt between the Rendalen and Moelv formations is further evidence for minor volume of magmatism coeval with sedimentation of the Hedmark Group (Furnes *et al.*, 1983).

Discussion

In the Varanger peninsula in Finmark, the reference Neoproterozoic

sequence contains two diamictite horizons in the Vestertana Group (Fig. 1a). These are the lower Smalfjorden Formation and the upper Mortensnes Formation (Edwards, 1984). The Smalfjorden formation is covered by a thin and discontinuous 'cap' dolostone, while the Mortensnes Formation is covered by a shale and sandstone sequence. Ediacaran fossils are reported above the Mortensnes Formation (Farmer *et al.*, 1992). The timing of deposition of the diamictites is estimated between *c.* 630 and 560 Ma, with Rb–Sr data on illite from shale horizons bracketing the glacial deposits (Gorokhov *et al.*, 2001). The occurrence of detrital (pre-diagenesis) and metamorphic (post-diagenesis) illite in the dated samples nevertheless illustrates the difficulty to obtain reliable deposition ages. On the basis of sequence stratigraphy, the Moelv Formation in the Hedmark Group is generally correlated with the Mortensnes Formation (Vidal and Moczydlowska, 1995; Harland, 1997; Evans, 2000). No 'cap' carbonate horizon is reported above the Moelv Tillite. An unpublished whole-rock Rb–Sr isochron age of 612 ± 18 Ma for the Ekre shale was quoted by Vidal and Moczydlowska (1995). The geological significance of this date is difficult to judge. The date of 620 ± 14 Ma obtained in this study represents a first reliable maximum age for deposition of the Moelv Tillite. If the correlation between the Mortensnes and Moelv Formations is accepted, it defines a maximum age for the youngest recorded Neoproterozoic Varanger glaciation in Baltica.

Available dates on accepted Marinoan glacial deposits worldwide includes a bracket of 663 ± 4 to 599 ± 4 Ma for the Nantuo Formation in south China (Zhou *et al.*, 2004), a Re–Os date of 608 ± 5 Ma for the post-glacial Old Fort Point Formation in western Canada (Kendall *et al.*, 2004), and a U–Pb date of 636 ± 1 Ma on a volcanic interlayer in the Ghaub Formation, Namibia (Hoffman *et al.*, 2004). A maximum Re–Os age of 592 ± 14 Ma for the Olympic Formation in central Australia (Schaefer and Burgess, 2003) is controversial. A minimum age of 601 ± 4 Ma suggests that the Port Askaig Tillite in the Argyll Group, Scotland, is related to the Marinoan event (Dempster *et al.*, 2002). If the 636 ± 1 Ma estimate is privileged, a correlation between the Moelv Tillite and other accepted Marinoan glacial deposits is poorly probable. Nevertheless, it cannot be strictly ruled out, as a global glaciation may last for several million years (Hoffman and Schrag, 2002).

There is stratigraphic and chemostratigraphic evidence on several continents for post-Marinoan Neoproterzoic glacial deposits (e.g. Grey and Corkeron, 1998; Xiao *et al.*, 2004). These deposits generally show a poorly developed 'cap' carbonate or lack it. Dated deposits include two formations from Avalonia, namely the Squantum Tillite in the Boston basin deposited between 595 ± 2 and *c.* 570 Ma (Thompson and Bowring, 2000), and the Gaskiers Formation in Newfoundland dated at *c.* 580 Ma by interlayered ash beds (Myrow and Kaufman, 1999; Bowring *et al.*, 2003). Although generally attributed to the Marinoan glaciation, the Croles Hill diamictite in the Togari Group, Tasmania, is younger than 582 ± 4 Ma (Calver *et al.*, 2004). Lithological and geochronological data are favourable to a correlation between the Moelv, Mortensnes, Squantum, Gaskiers and Croles Hill formations, reflecting a glaciation *c.* 580 Ma. Ediacaran fossils reported in sediments shortly overlying the Mortensnes and Gaskiers Formations share some morphological attributes, supporting a correlation (Farmer *et al.*, 1992; Bowring *et al.*, 2003).

Available palaeomagnetic data do not lead to a reliable Neoproterozoic

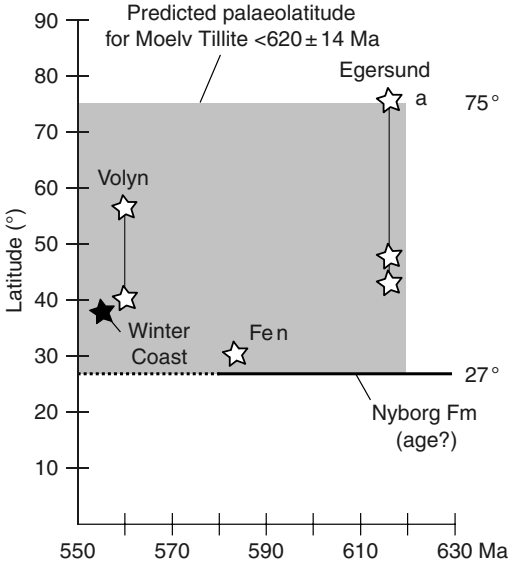

Fig. 3 Predicted palaeolatitudes for the Oslo Region (60°N, near the present day location of the Hedmark Group) based on selected palaeomagnetic poles discussed in the text. Egersund dolerite swarm: two poles listed in Torsvik *et al.* (1996) and the pole labelled with (a) is from Torsvik and Cocks (2005) and H.J. Walderhaug, T.H. Torsvik and E.A. Eide (unpublished data). Fen carbonatite complex: Meert *et al.* (1998). Volyn basalts: Glevasskaya *et al.* (2001) and Nawrocki *et al.* (2004). Winter Coast, White Sea: Popov *et al.* (2002). Nyborg interglacial Formation, Vestertana Group, Finnmark: Torsvik *et al.* (1995). The age of the Nyborg Formation is unknown and the palaeolatitude is therefore represented by a horizontal line. Both the Nyborg and Winter Coast data are derived from sediments and inclination shallowing, a well-known phenomena in sediments, might lead to erroneously low latitude for these poles. Some authors argue that the Fen pole represents a Permian overprint (e.g. Popov *et al.*, 2002; Eneroth and Svenningsen, 2004) as the Fen carbonatite complex is situated close to the Oslo magmatic rift. Note, however, that the late Silurian Ringerike sandstone, situated within the rift, yields a primary magnetic signature (stratigraphically linked reversals) and no isotopic systems (K–Ar, Rb–Sr, Pb–Pb) in rocks of the Fen complex are affected by Permian disturbances.

apparent polar wander path for Baltica (Torsvik, 2003). Palaeomagnetic data are confusing: stability tests are rare, rock age or remanence acquisition (primary vs. secondary) is often disputed, or unknown, and metamorphosed rocks now located in high Caledonian allochthons have been arguably used to position Baltica (e.g. Eneroth and Svenningsen, 2004). Palaeomagnetic data on non-allochtonous rocks formed during the time interval allowed for the Varanger glaciation, i.e. 620 ± 14 Ma to 542 Ma (Cambrian boundary), are reviewed hereafter (Fig. 3). Two published studies on the 616 ± 3 Ma Egersund dolerites, south Norway, yield palaeolatitudes for the Oslo region between 43° and 47° (listed in Torsvik *et al.*, 1996). A new study including positive contact tests and ^{40}Ar–^{39}Ar biotite ages close to the U–Pb intrusion age yields an improved palaeolatitude of 75° (Torsvik and Cocks, 2005; H.J. Walderhaug, T.H. Torsvik and E.A. Eide, unpublished data). The Fen carbonatite complex (south Norway) yields a local palaeolatitude of 30° at 583 ± 15 Ma (Meert *et al.*, 1998). Two studies on the Volyn basalts (Ukraine) and a study of the Vendian Winter Coast sediments (White Sea, Russia) yield latitudes for the Oslo region between 38 and 56° *c.* 560–550 Ma (Glevasskaya *et al.*, 2001; Popov *et al.*, 2002; Nawrocki *et al.*, 2004). Available data point to an intermediate to polar latitude position for Baltica between *c.* 620 and 555 Ma. These latitudes are consistent with cold to temperate climatic conditions, in accordance with widespread preservation of feldspar clasts in the Hedmark Group. The lack of reported 'cap' carbonate and gradational transition between the Moelv diamictite and the Ekre shale do not provide direct evidence for a dramatic climatic overturn at the end of the glaciation, as predicted in the 'Snowball Earth' model (Hoffman and Schrag, 2002). The palaeolatitude and stratigraphic evidence from the Hedmark Group are therefore compatible with a glaciation related to normal climatic variations as observed in the Phanerozoic (Evans, 2003). They do not rule out a global 'Snowball Earth' model, as this model allows for intermediate to high latitude glaciers and discontinuous 'cap' carbonate deposition. The most polar latitude estimate of 75°, based on the Egersund pole, if applicable, nevertheless refutes a model featuring changes in Earth's obliquity, as such a model precludes high-latitude glaciers.

Acknowledgements

This study was jointly funded by the Geological Survey of Norway and Macquarie University, Sydney. Norm Pearson, Suzy Elhlou and Elena Belousova are thanked for their contributions to the analytical work. D. Roberts read the manuscript. D.A.D. Evans and M. Thirlwall made constructive critical reviews. This is GEMOC contribution 386.

References

Andersen, T., Griffin, W.L. and Pearson, N.J., 2002. Crustal evolution in the SW part of the Baltic Shield: the Hf isotope evidence. *J. Petrol.*, **43**, 1725–1747.

Andersen, T., Griffin, W.L., Jackson, S.E., Knudsen, T.-L. and Pearson, N.J., 2004. Mid-Proterozoic magmatic arc evolution at the southwest margin of the Baltic shield. *Lithos*, **73**, 289–318.

Belousova, E.A., Griffin, W.L., Shee, S.R., Jackson, S.E. and O'Reilly, S.Y., 2001. Two age populations of zircons from the Timber Creek kimberlites, Northern Territory, as determined by laser-ablation ICP-MS analysis. *Aust. J. Earth Sci.*, **48**, 757–765.

Belousova, E.A., Griffin, W.L., O'Reilly, S.Y. and Fisher, N.I., 2002. Igneous zircon: trace element composition as an indicator of source rock type. *Contrib. Mineral. Petrol.*, **143**, 602–622.

Bingen, B. and Demaiffe, D., 1999. Geochemical signature of the Egersund basaltic dyke swarm, SW Norway, in the context of late-Neoproterozoic opening of the Iapetus ocean. *Norsk Geol. Tidsskr.*, **79**, 69–85.

Bingen, B., Demaiffe, D. and van Breemen, O., 1998. The 616 Ma old Egersund basaltic dike swarm, SW Norway, and late Neoprotorozoic opening of Iapetus ocean. *J. Geol.*, **106**, 565–574.

Bingen, B., Skår, Ø., Marker, M., Sigmond, E.M.O., Nordgulen, Ø., Ragnhildstveit, J., Mansfeld, J., Tucker, R.D. and Liégeois, J.-P., 2005. Timing of continental building in the Sveconorwegian orogen, SW Scandinavia. *Norw. J. Geol.*, **85**, 87–116.

Bjørlykke, K., Elvsborg, A. and Høy, T., 1976. Late Precambrian sedimentation in the central Sparagmite basin of South Norway. *Norsk Geol. Tidsskr.*, **56**, 233–290.

Bowring, S.A., Myrow, P.M., Landing, E., Ramezani, J. and Grotzinger, J., 2003. Geochronological constraints on terminal Neoproterozoic events and the rize of metazoans. *Geophys. Res. Abst.*, **5**, 13219.

Brasier, M.D., McCarron, G., Tucker, R.D., Leather, J., Allen, P.A. and Shields, G., 2000. New U-Pb zircon dates for the Neoproterozoic Ghubrah glaciation and for the top of the Huqf Supergroup, Oman. *Geology*, **28**, 175–178.

Calver, C.R., Black, L.P., Everard, J.L. and Seymour, D.B., 2004. U-Pb zircon age constraints on late Neoproterozoic glaciation in Tasmania. *Geology*, **32**, 893–896.

Dempster, T.J., Rogers, G., Tanner, P.W.G., Bluck, B.J., Muir, R.J., Redwood, S.D., Ireland, T.R. and Paterson, B.A., 2002. Timing of deposition, orogenesis and glaciation within the Dalradian rocks of Scotland: constraints from U-Pb zircon ages. *J. Geol. Soc. Lond.*, **159**, 83–94.

Edwards, M.B., 1984. Sedimentology of the Upper Proterozoic glacial record, Vestertana Group, Finnmark, North Norway. *Norges Geol. Unders. Bull.*, **394**, 1–76.

Eneroth, E. and Svenningsen, O.M., 2004. Equatorial Baltica in the Vendian: palaeomagnetic data from the Sarek Dyke Swarm, northern Swedish Caledonides. *Precambrian Res.*, **129**, 23–45.

Evans, D.A.D., 2000. Stratigraphic, geochronological and paleomagnetic constraints upon the Neoproterozoic climatic paradox. *Am. J. Sci.*, **300**, 347–433.

Evans, D.A.D., 2003. A fundamental Precambrian-Phanerozoic shift in earth's glacial style? *Tectonophysics*, **375**, 353–385.

Farmer, J., Vidal, G., Moczydlowska, M., Strauss, H., Ahlberg, P. and Siedlecka, A., 1992. Ediacaran fossils from the Innerelv Member (late Proterozoic) of the Tanafjorden area, northeastern Finnmark. *Geol. Mag.*, **129**, 181–195.

Furnes, H., Nystuen, J.P., Brunfelt, A.O. and Solheim, S., 1983. Geochemistry of Upper Riphean-Vendian basalts associated with the "Sparagmites" of S Norway. *Geol. Mag.*, **120**, 349–361.

Glevasskaya, A.M., Mikhailova, N.P. and Kravchenko, S.N., 2001. Paleomagnetism of the Volyn and Mogilev-Podolia Vendian series of the South-Western Part of the East-European platform. *Geophys. J.*, **20**, 149–175.

Gorokhov, I.M., Siedlecka, A., Roberts, D., Melnikov, N.N. and Turchenko, T.L., 2001. Rb-Sr dating of diagenetic illite in Neoproterozoic shales, Varanger Peninsula, northern Norway. *Geol. Mag.*, **138**, 541–562.

Grey, K. and Corkeron, M., 1998. Late Neoproterozoic stromatolites in

glacigenic successions of the Kimberley region, Western Australia: evidence for a younger Marinoan glaciation. *Precambrian Res.*, **92**, 65–87.

Griffin, W.L., Pearson, N.J., Belousova, E.A., Jackson, S.E., van Achterbergh, E., O'Reilly, S.Y. and Shee, S.R., 2000. The Hf isotope composition of cratonic mantle: LAM-MC-ICPMS analysis of zircon megacrysts in kimberlites. *Geochim. Cosmochim. Acta*, **64**, 133–147.

Griffin, W.L., Wang, X., Jackson, S.E., Pearson, N.J., O'Reilly, S.Y., Xu, X. and Zhou, X., 2002. Zircon chemistry and magma mixing, SE China: in-situ analysis of Hf isotopes, Tongulu and Pingtan igneous complexes. *Lithos*, **61**, 237–269.

Harland, W.B., 1997. *The Geology of Svalbard*. The Geological Society, London, Memoir.

Hoffman, P.F. and Schrag, D.P., 2002. The snowball Earth hypothesis: testing the limits of global change. *Terra Nova*, **14**, 129–155.

Hoffman, K.-H., Condon, D.J., Bowring, S.A. and Crowley, J.L., 2004. U-Pb zircon date from the Neoproterozoic Ghaub Formation, Namibia: constrains on Marinoan glaciation. *Geology*, **32**, 817–820.

Jackson, S.E., Pearson, N.J., Griffin, W.L. and Belousova, E.A., 2004. The application of laser ablation-inductively coupled plasma-mass spectrometry to in situ U-Pb zircon geochronology. *Chem. Geol.*, **211**, 47–69.

Kendall, B.S., Creaser, R.A., Ross, G.M. and Selby, D., 2004. Constraints on the timing of Marinoan "Snowball Earth" glaciation by 187Re-187Os dating of a Neoproterozoic, post-glacial black shale in Western Canada. *Earth Planet. Sci. Lett.*, **222**, 729–740.

Kumpulainen, R. and Nystuen, J.P., 1985. Late Proterozoic basin evolution and sedimentation in the westernmost part of Baltoscandia. In: *The Caledonide Orogen – Scandinavia and Related Areas* (D.G. Gee and B.A. Sturt, eds), pp. 213–232. John Wiley & Sons Ltd Chichester, UK.

Ludwig, K.R., 2001. *Users Manual for Isoplot/Ex Version 2.49, A Geochronological Toolkit for Microsoft Excel*. Special Berkeley Geochronology Center, Berkeley, CA, Special Publication No. 1a.

Meert, J.G., Torsvik, T.H., Eide, E.A. and Dahlgren, S., 1998. Tectonic significance of the Fen Province, S. Norway: constraints from geochronology and paleomagnetism. *J. Geol.*, **106**, 553–564.

Myrow, P.M. and Kaufman, A.J., 1999. A newly discovered cap carbonate above Varanger-age glacial deposits in Newfoundland, Canada. *J. Sed. Res.*, **69**, 784–793.

Nawrocki, J., Boguckij, A. and Katinas, V., 2004. New Late Vendian paleogeography of Baltica and the TESZ. *Geol. Q.*, **48**, 309–316.

Nystuen, J.P., 1981. The late Precambrian "Sparagmites" of southern Norway: a major Caledonian allochthon – The Osen-Røa Nappe Complex. *Am. J. Sci.*, **281**, 69–94.

Nystuen, J.P., 1987. Synthesis of the tectonic and sedimentological evolution of the late Proterozoic–early Cambrian Hedmark Basin, the Caledonian Thrust Belt, southern Norway. *Norsk Geol. Tidsskr.*, **67**, 395–418.

Nystuen, J.P. and Sæther, T., 1979. Clast studies in the Late Precambrian Moelv Tillite and Osdal Conglomerate, Sparagmite region, south Norway. *Norsk Geol. Tidsskr.*, **59**, 239–251.

Patchett, P.J., Kouvo, O., Hedge, C.E. and Tatsumoto, M., 1981. Evolution of continental crust and mantle heterogeneity: evidence from Hf isotopes. *Contrib. Mineral. Petrol.*, **78**, 279–297.

Popov, V., Iosifidi, A., Khramov, A., Tait, J. and Bachtadse, V., 2002. Paleomagnetism of Upper Vendian sediments from the Winter Coast, White Sea region, Russia: implications for the paleogeography of Baltica during Neoproterozoic times. *J. Geophys. Res.*, **107**, doi:10.1029/2001JB001607.

Schaefer, B.F. and Burgess, J.M., 2003. Re-Os isotopic age constraints on deposition in the Neoproterozoic Amadeuns Basin: implications for the 'Snowball Earth'. *J. Geol. Soc. Lond.*, **160**, 825–828.

Scherer, E., Munker, C. and Mezger, K., 2001. Calibration of the lutetium-hafnium clock. *Science*, **293**, 683–687.

Thompson, M.D. and Bowring, S.A., 2000. Age of the Squantum "tillite", Boston basin, Massachusetts: U-Pb zircon constraints on terminal Neoproterozoic glaciation. *Am. J. Sci.*, **300**, 630–655.

Torsvik, T.H., 2003. The Rodinia jigsaw puzzle. *Science*, **300**, 1379–1381.

Torsvik, T.H. and Cocks, L.R.M., 2005. Norway in space and time: a Centennial Cavalcade. *Norw. J. Geol.*, **85**, 73–86.

Torsvik, T.H., Lohmann, K.C. and Sturt, B.A., 1995. Vendian glaciations and their relation to the dispersal of Rodinia: Paleomagnetic constraints. *Geology*, **23**, 727–730.

Torsvik, T.H., Smethurst, M.A., Meert, J.G., Van der Voo, R., Mc Kerrow, W.S., Brasier, M.D., Sturt, B.A. and Walderhaug, H.J., 1996. Continental break up and collision in the Neoproterozoic and Paleozoic – A tale of Baltica and Laurentia. *Earth Sci. Rev.*, **40**, 229–258.

Vervoort, J.D. and Patchett, P.J., 1996. Behavior of hafnium and neodymium isotopes in the crust: contraints from Precambrian crustally derived granites. *Geochim. Cosmochim. Acta*, **60**, 3717–3733.

Vidal, G. and Moczydlowska, M., 1995. The Neoproterozoic of Baltica – stratigraphy, palaeobiology and general geological evolution. *Precambrian Res.*, **73**, 197–216.

Wiedenbeck, M., Allé, P., Corfu, F., Griffin, W.L., Meier, M., Oberli, F., Von Quadt, A., Roddick, J.C. and Spiegel, W., 1995. Three natural zircon standards for U-Th-Pb, Lu-Hf, trace element and REE analyses. *Geostandards Newsl.*, **19**, 1–23.

Williams, G.E., 1975. Late Precambrian glacial climate and the Earth's obliquitiy. *Geol. Mag.*, **112**, 441–465.

Xiao, S., Bao, H., Wang, H., Kaufman, A.J., Zhou, C., Li, G., Yuan, X. and Ling, H., 2004. The Neoproterozoic Quruqtagh Group in eastern Chinese Tianshan: evidence for a post-Marinoan glaciation. *Precambrian Res.*, **130**, 1–26.

Zhou, C., Tucker, R.D., Xiao, S., Peng, Z., Yuan, X. and Chen, Z., 2004. New constraints on the ages of Neoproterozoic glaciations in south China. *Geology*, **32**, 437–440.

Received 16 September 2004; revised version accepted 7 January 2005

